SUPPORTING INFORMATION

Physical and Structural Characterization of Imidazolium Based Organic-Inorganic Hybrid: $(C_3N_2H_5)_2[CoCl_4]$

Anna Piecha-Bisiorek, Alina Bieńko, Ryszard Jakubas, Roman Boča, Marek Weselski, Vasyl Kinzhybalo, Adam Pietraszko, Martyna Wojciechowska, Wojciech Medycki and Danuta Kruk

e-mail: anna.piecha@chem.uni.wroc.pl

TABLE OF CONTENS:

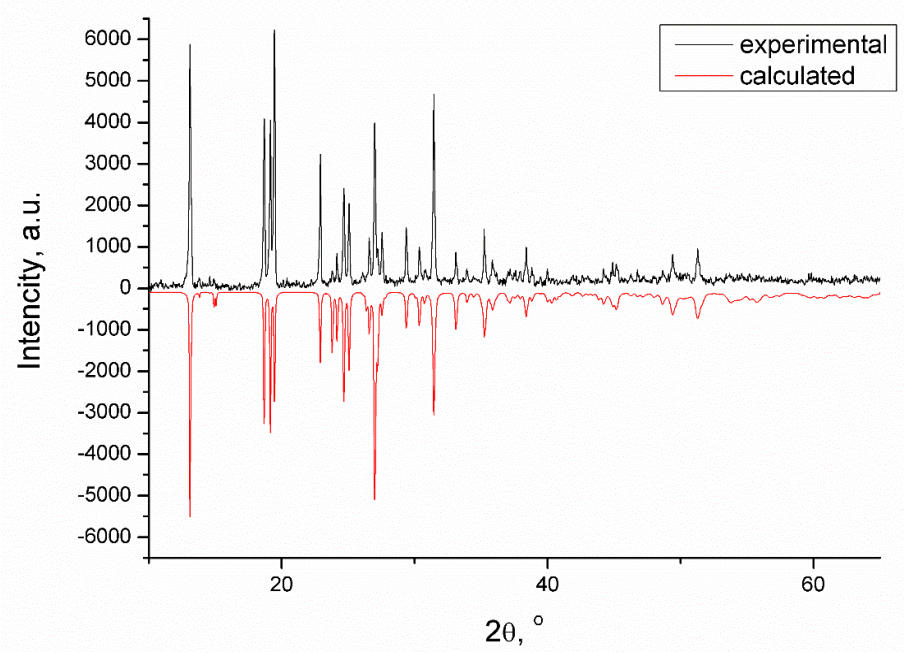

Fig. S1 X-ray diffraction pattern of **ICC** at 295 K.

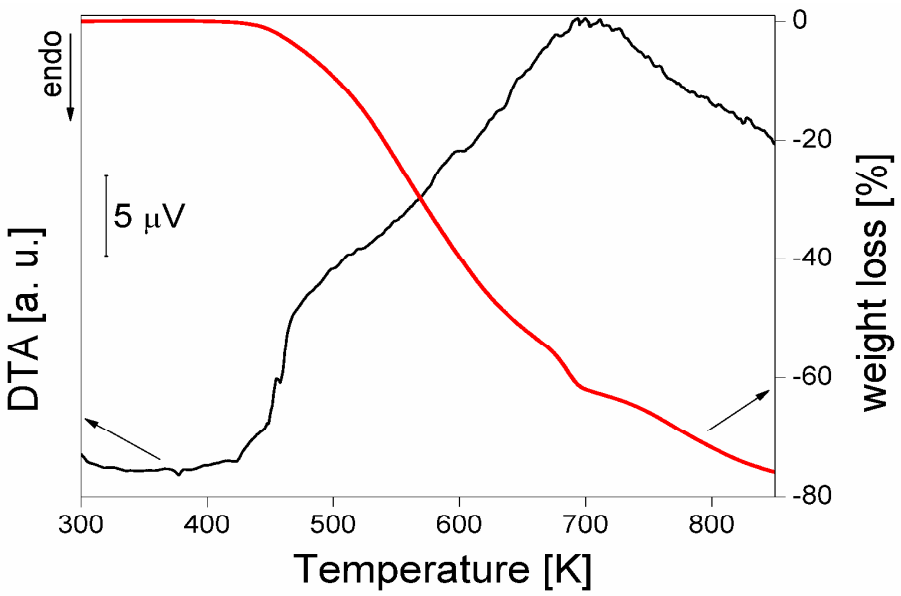

Fig. S2 Simultaneous thermogravimetric analysis and differential thermal analysis scan (with the ramp rate of 2 K min^{-1}, sample mass 10.622 mg) for the **ICC** crystal.

AC measurement

The AC susceptibility data was taken at T = 1.9 K for a set of frequencies in dependence upon the applied dc field. The data presented in Fig. S3 indicates a rather complex behaviour because the out-of-phase components do not follow a simple trend.

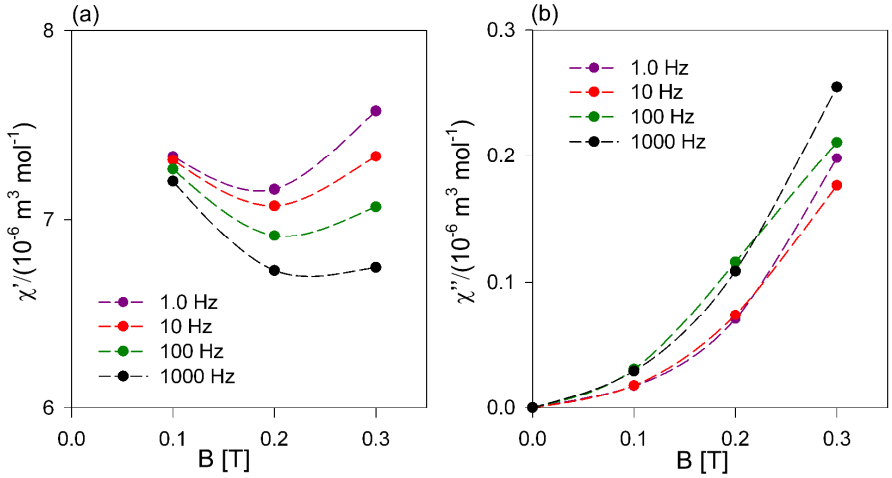

Fig. S3 Field dependence of the AC susceptibility components at T = 1.9 K for a set of frequencies of the AC field.

The AC susceptibility data was also sorted according to the temperature and plotted as functions of the frequency f of the AC field: χ' vs f and χ'' vs f, respectively (Fig. S4).

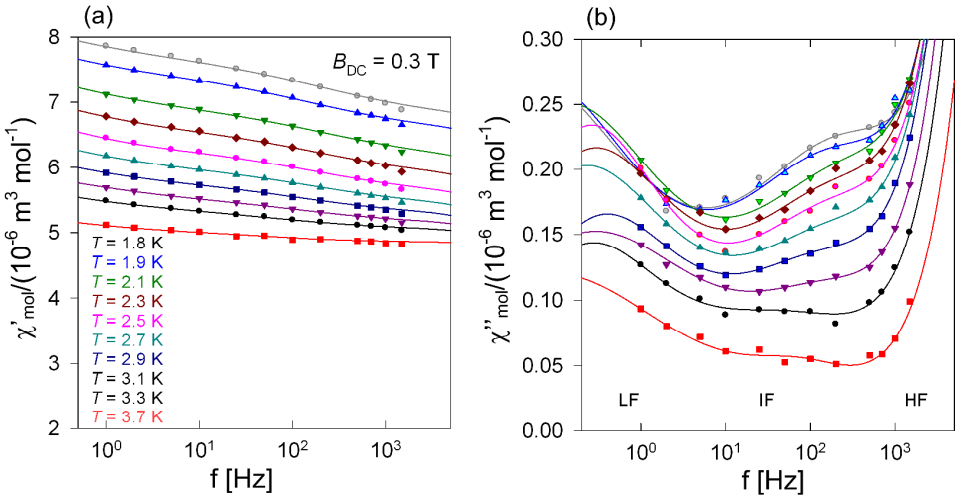

Fig. S4 In-phase (a) and out-of-phase (b) components of the AC susceptibility as functions of the frequency of the AC field at the constant temperature. Lines – fitted.

It can be seen that three relaxation processes coexist, each at the different window of frequencies. The intermediate-frequency (IF) process is characterized by a central peak that is followed by an on-set of the high-frequency process (HF) on right side, and the on-set of the low-frequency (LF) process at the left side of Figure S4. Each process (peak) is characterized by the peak position f''_{max} (inversely proportional to the relaxation time $\tau=1/(2\pi f''_{max})$), height (given by the isothermal susceptibility χ_T) and the width (related to the distribution parameter α). Usually 12 data of χ' and 12 data for χ'' could be sufficient to do a fitting with 9

parameters with a three-component extended Debye function. However, the actual data set does not allow a reliable determination of the LF and HF processes because the maximum of χ'' lies outside the hardware limits. Also the adiabatic susceptibility χ_S (the high-frequency limit) cannot be determined with this data set. For this reasons the fitted parameters listed in Tab. 1 must be considered only as rough estimates.

Tab. S1 Parameters of the extended three-component Debye model for ICC using data taken at BDC =0.3T.[a]

T [K]	χ_{T1}	α_1	τ_1 [s]	χ_{T2}	α_2	τ_2 [10^{-3} s]	χ_{T3}	τ_3 [10^{-6} s]	$R(\chi')$	$R(\chi'')$
1.8	1.51	0.57	4.43	2.44	0.50	0.65	9.15	1.53	0.40	1.9
1.9	1.33	0.53	3.00	2.21	0.50	0.84	8.72	2.10	0.28	2.4
2.1	1.15	0.50	1.33	1.97	0.50	0.61	8.05	2.19	0.30	1.6
2.3	0.91	0.46	0.72	1.62	0.47	0.73	7.46	2.61	0.39	1.7
2.5	0.82	0.38	0.71	1.55	0.49	0.81	7.11	2.58	0.35	1.7
2.7	0.86	0.47	0.83	1.44	0.47	0.81	6.83	2.85	0.35	1.6
2.9	0.60	0.41	0.50	1.11	0.47	1.10	6.36	3.00	0.34	0.9
3.1	0.79	0.54	0.65	1.09	0.40	0.93	6.23	2.71	0.26	1.1
3.3	0.50	0.38	0.72	0.86	0.50	2.36	5.88	2.34	0.29	2.9
3.7	0.69	0.57	1.74	0.78	0.23	1.92	5.62	1.72	0.39	4.5

[a] Fixed $\chi_S = 0$ and $\alpha_3 = 0$; SI unit for the molar magnetic susceptibility [10^{-6} m^3 mol^{-1}]. $R(\chi')$ and $R(\chi'')$ – Discrepancy factors. Two components of the magnetic susceptibility.

a) in phase (Eq. 5):

$$\chi'(\omega) = \chi_S + (\chi_{T1} - \chi_S)\frac{1 + (\omega\tau_1)^{1-\alpha_1}\sin(\pi\alpha_1/2)}{1 + 2(\omega\tau_1)^{1-\alpha_1}\sin(\pi\alpha_1/2) + (\omega\tau_1)^{2-2\alpha_1}}$$
$$+(\chi_{T2} - \chi_{T1})\frac{1 + (\omega\tau_2)^{1-\alpha_2}\sin(\pi\alpha_2/2)}{1 + 2(\omega\tau_2)^{1-\alpha_2}\sin(\pi\alpha_2/2) + (\omega\tau_2)^{2-2\alpha_2}}$$
$$+(\chi_{T3} - \chi_{T2})\frac{1 + (\omega\tau_3)^{1-\alpha_3}\sin(\pi\alpha_3/2)}{1 + 2(\omega\tau_3)^{1-\alpha_3}\sin(\pi\alpha_3/2) + (\omega\tau_3)^{2-2\alpha_3}}$$

b) out of chase (Eq. 6):

$$\chi''(\omega) = (\chi_{T1} - \chi_S)\frac{(\omega\tau_1)^{1-\alpha_1}\cos(\pi\alpha_1/2)}{1+2(\omega\tau_1)^{1-\alpha_1}\sin(\pi\alpha_1/2)+(\omega\tau_1)^{2-2\alpha_1}}$$

$$+(\chi_{T2} - \chi_{T1})\frac{(\omega\tau_2)^{1-\alpha_2}\cos(\pi\alpha_2/2)}{1+2(\omega\tau_2)^{1-\alpha_2}\sin(\pi\alpha_2/2)+(\omega\tau_2)^{2-2\alpha_2}}$$

$$+(\chi_{T3} - \chi_{T2})\frac{(\omega\tau_3)^{1-\alpha_3}\cos(\pi\alpha_3/2)}{1+2(\omega\tau_3)^{1-\alpha_3}\sin(\pi\alpha_3/2)+(\omega\tau_3)^{2-2\alpha_3}}$$

The parameters resulted from the fitting procedure were used in constructing interpolation/extrapolation lines that allow construction of the Argand diagram (**Fig. S5**).

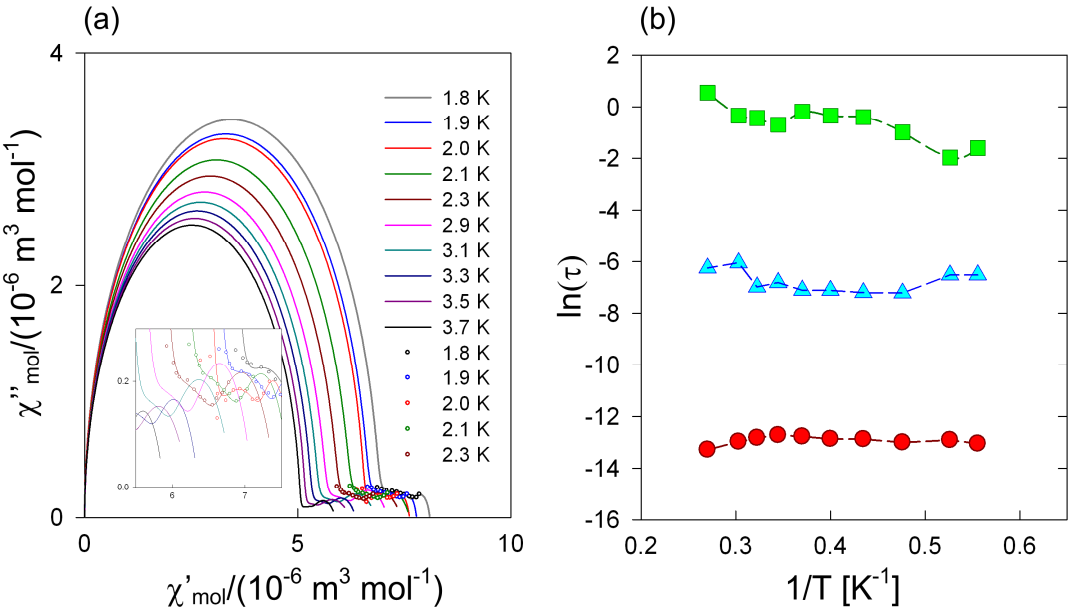

Fig. S5 (a) Argand (Cole-Cole) diagram for the AC susceptibility; (b) – Arrhenius-like plot.